



Industrial Microbiology

Isolation and expression of two polyketide synthase genes from *Trichoderma harzianum* 88 during mycoparasitism



Lin Yao^a, Chong Tan^c, Jinzhu Song^b, Qian Yang^b, Lijie Yu^a, Xinling Li^{a,*}

^a Key Laboratory of Molecular and Cytogenetics and Genetic Breeding of Heilongjiang Province, Harbin Normal University, Harbin, PR China

^b Department of Life Science and Engineering, Harbin Institute of Technology, Harbin, PR China

^c Research Center on Life Sciences and Environmental Sciences, Harbin University of Commerce, Harbin, PR China

ARTICLE INFO

Article history:

Received 10 August 2013

Accepted 5 September 2014

Available online 2 March 2016

Associate Editor: Eleni Gomes

Keywords:

Polyketide synthase

Real time quantitative PCR

Gene disruption

Fungal plant pathogens

ABSTRACT

Metabolites of mycoparasitic fungal species such as *Trichoderma harzianum* 88 have important biological roles. In this study, two new ketoacyl synthase (KS) fragments were isolated from cultured *Trichoderma harzianum* 88 mycelia using degenerate primers and analysed using a phylogenetic tree. The gene fragments were determined to be present as single copies in *Trichoderma harzianum* 88 through southern blot analysis using digoxigenin-labelled KS gene fragments as probes. The complete sequence analysis in formation of *pksT-1* (5669 bp) and *pksT-2* (7901 bp) suggests that *pksT-1* exhibited features of a non-reducing type I fungal PKS, whereas *pksT-2* exhibited features of a highly reducing type I fungal PKS. Reverse transcription polymerase chain reaction indicated that the isolated genes are differentially regulated in *Trichoderma harzianum* 88 during challenge with three fungal plant pathogens, which suggests that they participate in the response of *Trichoderma harzianum* 88 to fungal plant pathogens. Furthermore, disruption of the *pksT-2* encoding ketosynthase–acyltransferase domains through *Agrobacterium*-mediated gene transformation indicated that *pksT-2* is a key factor for conidial pigmentation in *Trichoderma harzianum* 88.

© 2016 Sociedade Brasileira de Microbiologia. Published by Elsevier Editora Ltda. This is an open access article under the CC BY-NC-ND license (<http://creativecommons.org/licenses/by-nc-nd/4.0/>).

Introduction

Biological control is an efficient and environmentally friendly way to prevent damping off. *Trichoderma* spp. are opportunistic biological control agents and avirulent plant symbionts.

T. harzianum belonging to *Trichoderma* spp. is widely used as a biopesticide and biofertilizer to control diseases and promote positive physiologic responses in plants. It combats several plant pathogenic fungi such as *Fusarium oxysporum* in bean and melon,^{1,2} *Botrytis cinerea* in tobacco,³ *Rhizoctonia solani* in cucumber,⁴ sheath blight in rice,⁵ creeping bentgrass and

* Corresponding author.

E-mail: qianyangcn@yeah.net (X. Li).

<http://dx.doi.org/10.1016/j.bjm.2016.01.004>

1517-8382/© 2016 Sociedade Brasileira de Microbiologia. Published by Elsevier Editora Ltda. This is an open access article under the CC BY-NC-ND license (<http://creativecommons.org/licenses/by-nc-nd/4.0/>).

tomato and *Sclerotinia sclerotiorum* in soybean.^{6–8} These reports suggest that *T. harzianum* strains parasitize a large variety of phytopathogenic fungi. It can also be used to control *R. solani*.⁹ Therefore, the molecular biocontrol mechanism of *T. harzianum* deserves further study. *T. harzianum* is reportedly effective in controlling fungi through different mechanisms, such as by inducing systemic resistance in plants, parasitizing other fungi by recognizing signals from the host to provoke the transcription of mycoparasitism-related genes, enzyme production and secretion, competing for nutrients and light and by producing antifungal metabolites.¹⁰ Harman et al.¹¹ reported that *T. harzianum* strains significantly enhance the systemic resistance and seed growth of maize, and induces the expression of proteins related to systemic induced resistance and increases growth.¹² Furthermore, although the underlying mechanism is much more complex than previously considered, the symbiosis-like interaction can be genetically improved to benefit plants more.¹³ Proteins such as G-proteins and mitogen-activated protein kinases affect biocontrol-relevant processes in the mycoparasitic interactions between *Trichoderma* and plant pathogens, such as the production of hydrolytic enzymes and antifungal metabolites and the formation of infection structures.¹⁴ The transcriptional factor Pac1 regulates some proteins involved in antagonism, such as chit42 chitinase, papA protease, gtt1 glucose permease, and qid74 cell wall protein.¹⁵ Competition for nutrients and space is also considered antagonism. *T. harzianum* showed dominance over *Alternaria alternata* under different environmental conditions (water activity and temperature).¹⁶ However, an in vitro antagonism test indicates that the production of antifungal compounds under nutrient-limiting conditions also contributes to fungistasis.¹⁷ In general, elucidating the pathogen-induced biocontrol mechanism of *T. harzianum* enables its application in controlling plant diseases. *T. harzianum* is currently used as a biofungicide to control *F. oxysporum* and *Sclerotium rolfsii* efficiently.¹⁸

Antifungal metabolites isolated from *Trichoderma* spp., including non-ribosomal peptides, polyketides, terpenoids and pyrones, play the important role in biological control.¹⁰ And studying biological activities, especially their biosynthetic pathway of those compounds is necessary for uncovering their biological control mechanisms.

Polyketide synthases (PKSs) are major enzymes in plants, fungi, and bacteria that are responsible for polyketide biosynthesis.¹⁹ Fungal PKSs are generally large multidomain systems that comprise a minimal set of ketosynthase, acyltransferase and acyl carrier protein domains. Type I PKSs elongate their polyketide products iteratively. In addition, ketoreductase, dehydratase and enoyl reductase domains may catalyse optional β -keto processing reactions, and optional accessory domains provide cyclase activity and methyl transferase activity.²⁰ Type I fungal PKSs are grouped into three classes based on their optional processing domains: non-reducing (e.g., melanin, aflatoxin), partially reducing (e.g., 6msas, calicheamicin), and highly reducing PKSs (e.g., T-toxin, fumonisins).^{8,21}

A variety of fungal polyketide synthase genes have been identified in recent ten years. However, there were no related research reports that polyketide synthase genes of *T. harzianum* were cloned and identified. In this study, the genes

encoding type I PKSs from *T. harzianum* mycelia were isolated using gene walking technology, and predictive analysis of its structure and encoding product. And PKS genes expression from different growth stages of antagonism between *T. harzianum* and fungal pathogens was detected by real-time quantitative RT-PCR (RT-qPCR) method. Furthermore, PKS gene function was studied by gene knockout technology. These studies were foundation for further revealed PKS in the role of biological metabolic process and its biological activity, and also provide new research ideas for future study of other fungi PKS gene.

Materials and methods

Fungal strains

The biocontrol agent *T. harzianum* strain 88 (CGMCC 5403; GenBank accession no. of ITS: JN579713) and the fungal plant pathogens *Rhizoctonia solani* (ACCC 36246), *S. sclerotiorum* (ACCC 36462) and *F. oxysporum* (ACCC 36966) were stored at the Microbial Genetic Engineering Laboratory, Harbin Institute of Technology (Harbin, China).

Isolation of PKS genes via gene walking using degenerate primers

Total DNA was isolated from *T. harzianum* 88 using a DNeasy Plant Mini kit (Invitrogen, Carlsbad, CA, USA). PKS ketoacyl synthase (KS) and acyltransferase (AT) sequences were amplified using the ketosynthase–acyltransferase (KA) degenerate primers KAF1 and KAR1 previously designed and reported by Amnuaykanjanasin et al.²² The PCR cycling conditions were as follows: 94 °C for 5 min; 30 cycles of 94 °C for 30 s, 58 °C for 30 s and 72 °C for 30 s; and 72 °C for 7 min. The resulting 700 bp product was gel isolated and inserted into the pMD18-T Easy vector (Promega, Madison, WI, USA). The recombinant vector was then transformed into competent *Escherichia coli* DH5 α (TaKaRa, Osaka, Japan) using the heat shock method.²³ The transformants were spread onto LB agar medium (1% tryptone, 0.5% yeast extract, 1% NaCl and 1.5% agar at pH 7.0) (TaKaRa, Osaka, Japan) containing ampicillin (100 μ g/mL) (TaKaRa, Osaka, Japan), X-Gal (0.2 mM) (TaKaRa, Osaka, Japan) and isopropylthio- β -galactoside (40 μ g/mL) (TaKaRa, Osaka, Japan) and incubated overnight at 37 °C. White colonies were selected for PCR identification.

The forward primer xKAF1 was designed based on the amino acid (aa) sequences in the conserved KS domain of reducing fungal PKS. The xKAF1 forward and KAR2 reverse primers were used to isolate an 800 bp fragment, which was cloned into the pMD18-T Easy vector (Promega, Madison, WI, USA) and sequenced.

A set of sense primers for 3' end amplification and anti-sense primers for 5' end amplification were designed for gene walking to obtain more complete genomic sequences of the two PKS genes. The reverse primers AP1, AP2, AP3 and AP4 for the two PKS genes were synthesized by TaKaRa (Osaka, Japan). The sequences of all primers used in this study are listed in the Online Resource 1. The fragment sequences were assembled by Phrap (<http://www.phrap.org/>)

and were then analysed using the BLASTx algorithm (<http://www.ncbi.nlm.nih.gov/BLASTx/>) and ORF finder (<http://www.ncbi.nlm.nih.gov/gorf/gorf.html>). The putative PKSs were designated as *pksT*.

Southern blot analysis

Two specific primer pairs were designed according to the KS domain fragment sequences, as shown in the schematic provided in the Online Resource 1. The DIG-labelled DNA probes *pksT-a-S* and *pksT-b-S* were generated from the cloned KS domain PCR products using a DIG-High Prime Labelling Mix (Roche Applied Sciences, Basel, Switzerland). Approximately 180 µg of genomic DNA was divided into six equal portions and digested overnight at 37 °C with the restriction enzymes BglII (used to digest two portions), HindIII, Sall or SacI (Promega, Madison, WI, USA) to ensure complete digestion. The digested genomic DNA was then electrophoresis on 0.7% (w/v) agarose gel (30 V, 12 h) and transferred onto positively charged nylon membranes (GE Healthcare, London, UK). The membranes were hybridized at 42 °C using the DIG-labelled probes *pksT-a-S* and *pksT-b-S* (sequences provided in Online Resource 2) and were detected with the DIG Luminescent Detection System (Roche Applied Sciences, Basel, Switzerland).

Reverse transcription-polymerase chain reaction (RT-PCR) of PKS genes

T. harzianum 88 mycelia (100 mg) were ground into powder after freezing in liquid nitrogen. RNA was then extracted using an RNeasy Plant Mini kit (Invitrogen, Carlsbad, CA, USA) and used for first-strand cDNA synthesis with SuperScriptII reverse transcriptase (Invitrogen, Carlsbad, CA, USA). The full cDNA sequence of *T. harzianum* 88 *pksT* was amplified using RT-PCR primers specific for *pksT-1* and *pksT-2* (Online Resource 1). The amplified fragments were then assembled using the program Phrap (<http://www.phrap.org/>).

The potential open reading frames (ORFs) of the two PKSs were scanned using FGENESH as the matrix (<http://linux1.softberry.com>) and compared with *T. vires* gene sequences. The conserved PKS domains were verified using CDD Search/PRS-BLAST (<http://www.ncbi.nlm.nih.gov/Structure/cdd/wrpsb.cgi>). The *pksT* KS domains were aligned with 55 fungal PKS protein sequences (reducing and non-reducing) retrieved from GenBank, and the two alignments analysed using CLUSTALW were embedded in the MEGA 4.0 program (<http://www.megasoftware.net/>). Bootstrap analysis was conducted using the MEGA 4.0 program with 1000 replications to obtain the confidence value for the aligned sequence dataset. A phylogenetic tree was constructed via maximum parsimony. The resultant phylogenetic tree was rooted in animal fatty acid synthase (*Gallus gallus* FAS), as previously described.²¹ The candidate secondary metabolite product was predicted using Natural Product Domain Seeker (NaPDos) (http://npdomainseeker.sdsc.edu/run_analysis.html).

Differential expression of PKS genes

RT-qPCR was used to evaluate the relative changes in gene expression in *T. harzianum* 88 during challenge with the

fungal pathogens *R. solani*, *S. sclerotiorum* and *F. oxysporum*. *T. harzianum* 88 was challenged with *R. solani*, *S. sclerotiorum* and *F. oxysporum* on plates using the procedure described by Carsolio et al.²⁴ Agar with cut fungal colonies were placed on opposite sides of 9 cm plates containing minimum medium (MM) with 2% agar and 2% glucose (Promega, Madison, WI, USA) and were covered with sterile cellophane sheets (Promega, Madison, WI, USA). *T. harzianum* 88 mycelia were collected when they touched the fungal pathogen at 3, 6, 12, 24, and 36 h. The procedure was repeated three times; however, only *Trichoderma* mycelia without spores and 0.5 cm away from the original inocula were collected. The control plate was *T. harzianum* 88 challenged with *T. harzianum* 88 mycelia, which were collected when the colonies touched each other (3, 6, 12, 24, and 36 h). The fungi were allowed to grow at 28 °C in the dark. Two primer pairs were selected for real-time RT-PCR analysis (Online Resource 1).

Total RNA was extracted from the mycelia and digested with DNase I (TaKaRa, Osaka, Japan).²⁵ Total RNA (4 µg) from each pooled sample was reverse transcribed into cDNA in the presence of oligo (dT) in a total volume of 25 µL. The synthesized cDNA was diluted with 25 µL of RNase-free ddH₂O and used as the template for RT-qPCR. Three pairs of primers were designed according to the ITS DNA from *R. solani*, *S. sclerotiorum*, and *F. oxysporum* to avoid the amplification of host fragments. Consequently, no fragments were amplified from cDNA templates. β -Tubulin (DY762540) transcripts were used as endogenous references for RT-qPCR. The primer set for β -tubulin was designed (additional data are given in the Online Resource 1) and RT-qPCR was performed using the SYBR[®] Premix Ex Taq[™] II (TaKaRa, Osaka, Japan) on an ABI Model 7500 HT sequence detector (ABI, Harbin Institute of Technology, China). Reagent mixes were prepared by combining 12.5 mL of SYBR[®] Premix Ex Taq[™] II (2 \times) with 2.5 µL of cDNA, 0.4 pmol/µL forward primers, 0.4 pmol/µL reverse primers, and 8 µL distilled water per reaction. The 25 µL reactions were carried out using programmed thermal cycling conditions consisting of 30 s at 95 °C, followed by 40 cycles of 5 s at 95 °C and 40 s at the appropriate annealing temperature for each real-time RT-PCR primer set. Three technical replicates of each of the three biological replicates were used to normalize the relative quantification analysis. Data from the threshold cycles were analysed according to the 2 ($\Delta\Delta C(T)$) methods in PKS gene expression.²⁶

A Student's t-test was used to determine whether the *pksT* genes significantly affected the survival of *T. harzianum* 88 with and without challenge from the three fungal plant pathogens. The level of significance of Student's t-test was set to $p < 0.05$ and was noted at $p < 0.01$.

Determination of optimal hygromycin B concentration

The wild type isolate (T) was assayed for growth on hygromycin B (hyg) (Promega, Madison, WI, USA) to optimize the negative selection for subsequent transformations. Agar pieces from plate cultures of the isolate were used to inoculate M-100 plates amended with varying hyg concentrations. Individual wells were photographed after 3 days.⁸

Table 1 – The primers used in this study.

Primer	Orientation	Sequence (5'–3')
T2-P1	Forward	CCGCTCGAGTGCTCTCCCTATGCCACTTC
T2-P2	Reverse	CCCAAGCTTAGATACACACCTCCCTCTTCAC
T2-P3	Forward	CGCGGATCCGCTTGATTGAGATCCACAGG
T2-P4	Reverse	CTAGTCTAGA AAGGCTCGGGAGAGACCA

Construction of *pksT-2* disruptant strain

Standard molecular techniques were used to construct all plasmids using restriction enzymes (Promega, Madison, WI, USA), alkaline phosphatase and PCR reagents (TaKaRa Bio Inc., Otsu, Japan). The plasmids were purified using the MiniBEST Plasmid Purification Kit Ver.3.0 (QIAGEN, USA). The binary vector pPZPtK8.10 was from Gardiner and Howlett.²⁷

The 5'-flanking DNA (1.4 kb, 5' and 3') and 3'-flanking DNA (1.114 kb, 5' and 3') of *pksT-2* were amplified by PCR using *T. harzianum* 88 genomic DNA as the template. The primers used to amplify the 5'-flanking DNA were T2-P1 and T2-P2, whereas those for the 3'-flanking DNA were T2-P3 and T2-P4 (Table 1). The 3'-flanking DNA was digested using *Bam*HI and *Xba*I (Promega, Madison, WI, USA), and the digested fragment was ligated into the *Bam*HI and *Xba*I site of the pPZPtK8.10. The generated plasmid was designated as pPZPtK8.10-ΔLR. The 5'-flanking DNA was digested with *Xho*I and *Hind*III (Promega, Madison, WI, USA), and the digested fragment was ligated into the *Xho*I and *Hind*III (Promega, Madison, WI, USA) site of the pPZPtK8.10. The generated plasmid was designated as pPZPtK8.10-ΔRR-ΔLR. The hygromycin resistance gene *Hyg* was amplified via PCR using the plasmid pCSN43 (Fungal Genetics Stock Center, Kansas, USA) as a template and primers hpg cassette F and hpg cassette R (Online Resource 1). The DNA fragment and pPZPtK8.10-ΔRR-ΔLR were digested using *Hpa*I (Promega, Madison, WI, USA), and the digested fragment was ligated into the blunt-end restriction *Hpa*I site of the pPZPtK8.10-ΔRR-ΔLR vector, which was treated with alkaline phosphatase. The generated plasmid was designated as pPZPtK8.10-ΔpksT-2.

Fungal transformation

A. tumefaciens-mediated transformation of *T. harzianum* 88 was performed as described for other fungi with minor modifications. Briefly, *A. tumefaciens* carrying the plasmid DNA was grown on solid LB medium containing 50 μg/mL kanamycin and 50 μg/mL streptomycin (LB-ka-str) (Promega, Madison, WI, USA) at 28 °C for 24 h. Single colonies were inoculated into liquid (LB-ka-str) and incubated at 28 °C for 12 h. The bacterial culture was liquid induction medium (IM) (10 mM K₂HPO₄, 10 mM KH₂PO₄, 2.5 mM NaCl, 2 mM MgSO₄, 0.7 mM CaCl₂, 9 nM FeSO₄, 4 mM NH₄SO₄, 10 mM glucose, 40 mM 2-[N-morpholino] ethanesulfonic acid, pH 5.3, and 0.5% glycerol) containing 200 μM acetosyringone (4'-hydroxy-3',5'-dimethoxyacetophenone) AS (Promega, Madison, WI, USA) to an optical density of 0.15 at 660 nm.⁸ After cultivation of bacterial cells at 28 °C for 6 h, 1 × 10⁶ fungal conidia/mL was mixed with the bacterial suspension and spread onto filters placed on IM agar containing 200 μM AS. After 48 h of incubation at 28 °C, the filters were transferred to MM-hyg agar selection

medium containing 300 μg/mL cefotaxime (Wako Chemicals) to inhibit the growth of *A. tumefaciens* cell. The sample was frozen in liquid nitrogen and lyophilized. DNA was extracted based on the cetyl trimethyl ammonium bromide (CTAB) mini extraction method with slight modifications. The frozen samples were ground in a frozen pestle with liquid nitrogen. The finely ground mycelia were transferred into sterile centrifuge tubes and pre-warmed at 65 °C. DNA extraction buffer [100 mM Tris HCl (pH 8.0), 1.4 M NaCl, 50 mM EDTA (pH 8.0), and 2% CTAB] (Wako Chemicals USA, Inc.) was added to the mixture, mixed well and incubated with gentle shaking for 1 h in a 65 °C water bath. After incubation, an equal volume of chloroform: isoamyl alcohol (24:1, v/v) (Wako Chemicals USA, Inc.) was added gently to denature proteins and centrifuged for 10 min at 15,670 × *g* and 4 °C. The aqueous phase was transferred into a sterile tube and DNA was precipitated for 20 min with 0.6 volume of cold isopropanol (Wako Chemicals USA, Inc.) at 16,100 × *g* and 4 °C. The supernatant was poured off and the pellet was washed twice with cold 70% ethanol (Wako Chemicals USA, Inc.). Then, the pellet was air-dried at room temperature and suspended in TE buffer [10 mM Tris HCl (pH 8.0), 1 mM EDTA (pH 8.0)]. The sample was treated with RNase A (20 mg/mL) (TaKaRa, Osaka, Japan) at 40 ng/mL DNA and incubated for 1 h at 37 °C. Then, 1 μL of genomic DNA from the knockout candidate was used as the template for PCR amplification using specific primers (ΔpksT-2 check F and ΔpksT-2 check R (Online Resource 1) and the Taq enzyme (TaKaRa, Osaka, Japan).

Single correct homologous integration through replacement of the resident ΔpksT-2 with ΔpksT-2:: *hyg* was confirmed via Southern blot analysis. The primers for the ΔpksT-2-S probe in the Online Resource 1 and its sequence are provided in the Online Resource 2.

Results and discussion

Isolation of PKS genes via gene walking using degenerate primers

The PCR of the *T. harzianum* 88 genomic DNA using degenerate primers based on the KS-AT region yielded one fragment. The KA-series primers are described in Online Resource 1. The 700 bp *pksT-a-1* fragment was cloned into the pMD18-T Easy vector (Promega, Madison, WI, USA). The sequence was homologous to *Penicillium marneffei* PKSs (58% identity, GenBank accession no. XP.002151003) based on BLASTx searches against the NCBI/GenBank database. The *pksT-a-1* fragment, amplified using the KAF1/KAR1 primers, was a putative non-reducing PKS fragment. However, PCR using other KA primer pairs for HP-reducing PKSs and PR-reducing PKSs did not produce any DNA fragment. We designed xKAF1 and xKAF2 as forward primers from the conserved regions of KS domains to obtain highly reducing PKSs. PCR using the xKAF1/KAR2 primers revealed one product with the expected size (800 bp), *pksT-b-1*, which was highly similar to HP-reducing PKSs genes from *Talaromyces stipitatus* (57% similarity, GenBank accession no. XP.002478229.1) under BLASTx analysis. xKAF1 primer was derived from the aa sequence EM(S)HGTGTQ in the KS domain of HR-type PKSs, whereas xKAF2 primer was derived from

EAEQMDPQ, which is conserved among PR PKSs, but amplification using xKAF2/KAR1 and KAR2 primers did not produce any viable DNA fragment. Baker et al.²⁸ used a phylogenomic approach to study the PKS repertoire encoded in the genomes of *Trichoderma reesei*, *T. atroviride* and *T. virens*. They found only one PR PKS gene in *T. atroviride*. Therefore, *T. harzianum* may not express this class of PKS.

Aside from the two aforementioned sequences, no other sequences were obtained through gene walking even though different approaches were used to isolate further sequences. Therefore, a set of sense primers for 5' end and 3' end amplification was designed for gene walking (Online Resource 1). The sequences were obtained by overlapping the fragments isolated through degenerate PCR, and other fragments were generated using the gene walking primer sets. Finally, most of the 5' and 3' end regions of the putative PKSs were determined via gene walking amplification, and the putative β -ketoacyl synthase genes were identified through Blast searches. Two final PKS sequences, 7187 bp (*pksT-a*) and 10,976 bp (*pksT-b*), were obtained.

Detection of PKS gene copy numbers

T. harzianum 88 genomic DNA was isolated using DNeasy Plant Maxi columns. Southern blot analysis with the DIG-labelled *pksT-a* probe revealed a single 2.08 kb band after *Bgl* II cleavage and a 3.36 kb band after *Hind* III cleavage (Fig. 1). Similarly, Southern blot analysis using the DIG-labelled *pksT-b* probe yielded a 6.0 kb band after *Pst* I cleavage and a 4.2 kb band after *Sac* I cleavage (Fig. 1). These findings demonstrate that *pksT-a* and *pksT-b* were present as single copies in *T. harzianum* 88. The iterative type of PKS (iPKS) only poses a single copy of each

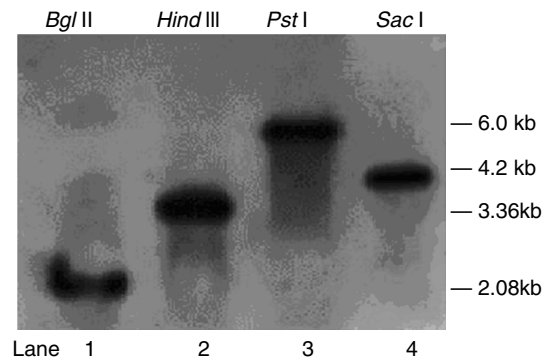


Fig. 1 – Southern blot analysis of genomic DNA from *T. harzianum* 88 digested with *Bgl* II, *Hind* III, *Pst* I or *Sac* I as indicated. Bands were detected with *pksT-a* (Lane 1, 2) and *pksT-b* (Lane 3, 4) digoxigenin-labelled probes.

catalytic domain, however these can be deployed repeatedly during synthesis of a single polyketide molecule. And single copies of the genome are most structural genes that carry out a variety various functions. Therefore, identification of specific gene copy number is important for in-depth understanding of its biological function.

Domain organization of PKS genes

Additional domain analysis was performed on *pksT-a* and *pksT-b* sequences after using degenerate primers and gene walking to obtain the two PKS gene fragments, which included two complete PKS fragments (*pksT-1* and *pksT-2*, respectively). A

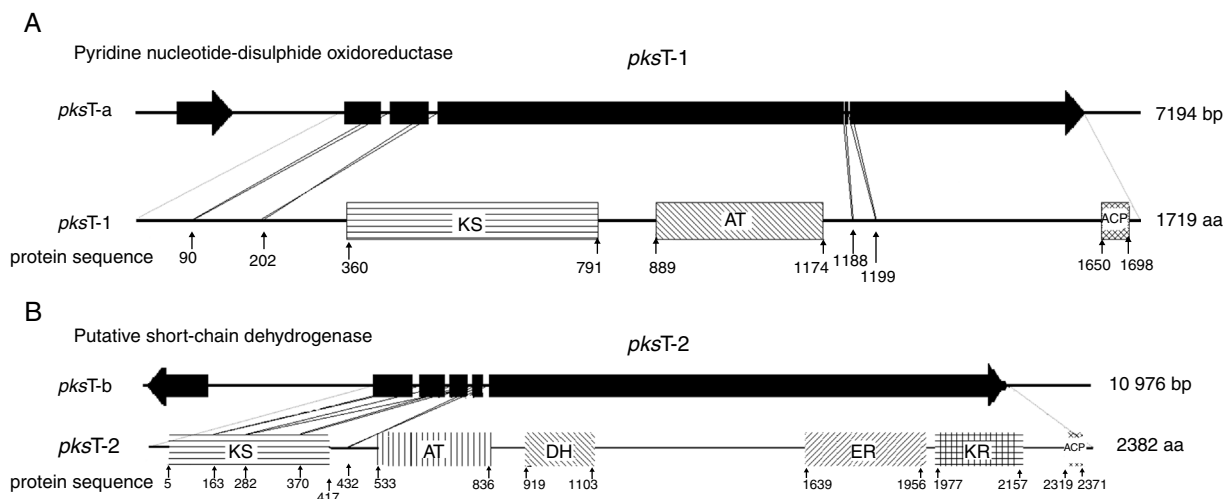


Fig. 2 – Structure and domain organization of *T. harzianum* 88 gene clusters. (A) *pksT-1* gene cluster structure in *T. harzianum* 88: two ORFs encoding a putative pyridine nucleotide-disulphide oxidoreductase, and *pksT-1*, respectively; *pksT-1* gene structure: the four introns are represented by lines and exons are represented by blocks. Schematic organization of the domains: KS, β -ketoacyl synthase (360–791), AT, acyltransferase (889–1174), ACP, acylcarrier protein (1650–1698). (B) *pksT-2* gene cluster structure in *T. harzianum* 88: two ORFs encoding a putative short-chain dehydrogenase, and *pksT-2*, respectively; *pksT-2* gene structure: the four introns are represented by lines and the exons are represented by blocks. Schematic organization of the domains: KS (5–417), AT (533–836), DH (919–1103), ER (1639–1956), KR (1977–2157) and ACP (2319–2371). The approximate domain boundaries were determined using the iterative PKS domain search program (http://www.nii.ac.in/~pkfdb/sbsp_ks/master.html).

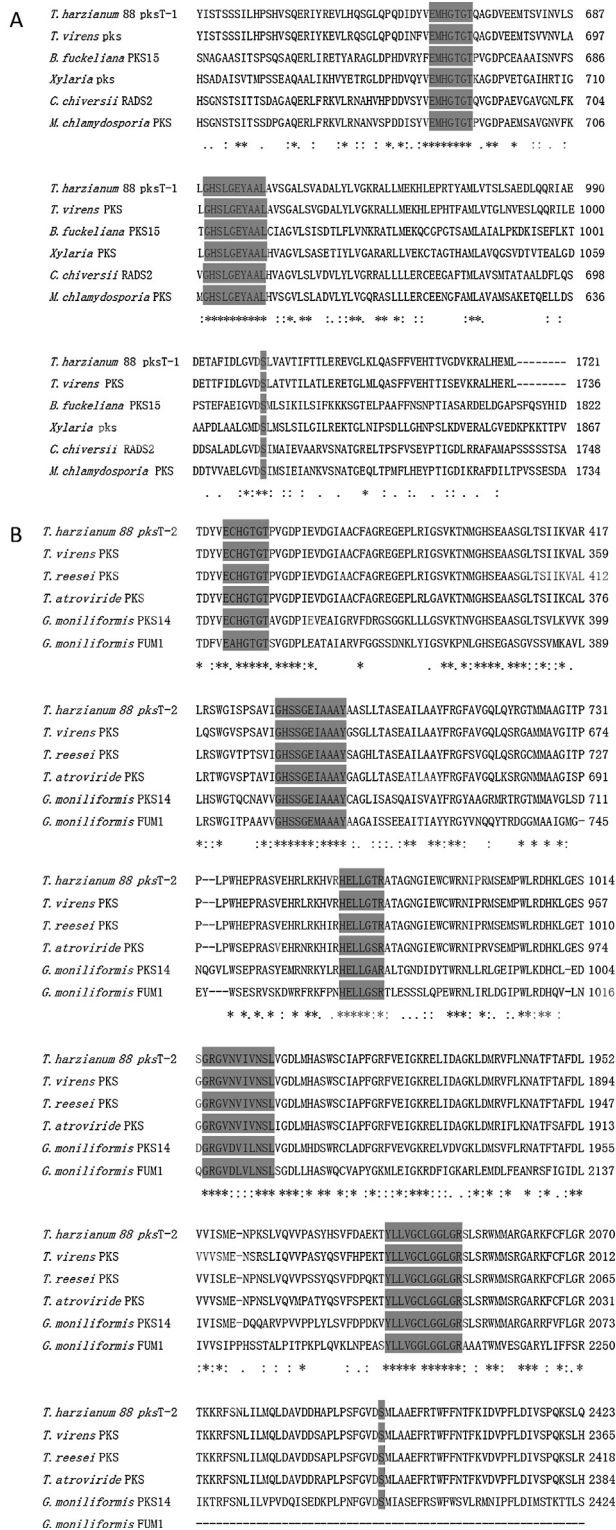


Fig. 3 – Alignment of *T. harzianum* 88 predicted PKS active regions with closely related fungal PKSs. (A) Alignment of putative catalytic motifs found in the deduced amino acid sequence of *T. harzianum* 88 *pksT-1* with those of *T. viresns* PKS (EHK16308.1); *B. fuckeliana* PKS15 (BAE80697.1); *Xylaria* sp. BCC 1067 PKS (ABB90283.1); *C. chiversii* RADS2 (ACM42403.1); *M. chlamydosporia* (ACD39770.1).

putative pyridine nucleotide–disulphide oxidoreductase gene clustered with *pksT-1* on the sequenced *pksT-a* fragment (Fig. 2A). Another gene was clustered with *pksT-2* on the *pksT-b* sequence, which was putatively identified as a short-chain dehydrogenase (Fig. 2B). The *pksT-1* sequence was deposited in the NCBI GenBank database under the accession number JN556039.1.

pksT-1, which contains 5669 bp and encodes a 1719 aa protein with three exons (positions 31–299, 354–639, 699–5306 from the transcript initial point), was confirmed via RT-PCR. The protein sequence of *pksT-1* contained the entire ancestral domain structure of type I non-reducing PKSs based on the presence of conserved motifs: KS (β -ketoacyl synthase)/AT/ACP. Comparison between the *pksT-1* protein sequence and the corresponding domains of other fungal PKSs showed conservation of the active site residues in KS (EMHGTGT), AT (GHSLGEYAAL) and ACP (GVDSLVL) (Fig. 3A). The *pksT-1* protein sequence was predicted to produce non-reduced non-cyclic PKS.²⁰

Another PKS gene, *pksT-2* is a 7901 bp gene that encodes a 2382 aa protein. The presence of five exons (positions 228–718, 766–1074, 1127–1337, 1399–1522 and 1590–7603 from the transcript initial point) was confirmed via RT-PCR. Six catalytic domains were identified in the *pksT-2* protein sequence based on the presence of conserved motifs. These domains, in order from the N-terminus to the C-terminus were KS, AT, DH, ER, KR and ACP. Comparison of the *pksT-2* protein sequence with the corresponding domains of other fungal PKSs showed conservation of the active site residues in KS (ECHGTGT), AT (GHSSGEIAAAAY), DH (HELLGTR), ER (GRGVNIVVNSL), KR (YLLVGCLGGLGR), and ACP (FGVDSML) (Fig. 3B). The *pksT-2* sequence was deposited in the NCBI GenBank database under accession number JN556040.1.

Phylogenetic analysis of the PKS fragments

The KS domain genealogy was used to infer the genealogy of type I fungal PKSs. Reliable sequences alignment of the proteins was impossible because of the insufficient similarity between members. The domains were group into previously established chemistry-based clades that represented non-reducing, partially reducing and highly reducing fungal PKSs based on a maximum parsimony phylogenetic analysis of the translated sequences. These three major clades were clustered into a larger clade of type I fungal PKSs, which is a sister clade of the FASs found in animals. In this present study, we chose several protein sequences from 3 *Trichoderma*

(B) Comparison with the highly conserved motifs of *T. harzianum* 88 *pksT-2*, *T. viresns* (EHK18438.1), *T. reesei* QM6a PKS (EGR47100), *T. atroviride* (EHK47038.1), *G. moniliformis* PKS14 (AAR92221.1) and *G. moniliformis* FUM1 (AAR92218.1). Amino acid residues conserved among all sequences are marked with an asterisk. Positions with conserved substitutions are marked with two dots, and those with semi-conserved substitutions are marked with one dot. Highlighted regions indicate the catalytic amino acid residues in the active site.

spp., 15 filamentous fungal species and *G. gallus* to construct a phylogenetic tree.

The full aa sequences of the KS domains from several reducing/non-reducing fungal PKSs were employed to generate a phylogenetic tree (Fig. 4). Phylogenetic analysis revealed that *pksT-1* was most closely related to the putative PKS from *T. vires* (80% similarity; GenBank accession no. EHK16308.1) and *Botryotinia fuckeliana* PKS15 (38% similarity; accession number AAR90251.1). *pksT-1* generated a dependent subclade that was close to the fungal non-reducing PKS clade II and III with strong bootstrap values (100%). These homologous proteins also contain the same domain organization as KS-AT-ACP in type I fungal PKSs. The KS-AT-ACP domain structure is universal in fungi, such as in *C. chiversii* RADS2 and *Metacordyceps chlamydosporia* PKSs, which are involved in RAL biosynthesis. The phylogenetic analysis demonstrated that *pksT-1* was more closely related to the PKSs involved in RAL biosynthesis than other known PKSs. RAL biosynthesis generally requires a non-reducing RADS2, a reducing PKS01, a halogenase and other cluster genes, but their functions are unknown.²⁹ Alignment of the two protein sequences using the NCBI-Blast2p algorithm showed that one gene from *T. vires* (accession number EHK16311.1), which encodes a reducing PKS, is most closely related to *C. chiversii* PKS01. The other protein from *T. vires* (accession number EHK16308.1) is highly similar to *C. chiversii* RADS2 based on Blast2p alignment. Therefore, *T. vires* likely has a similar gene cluster structure for RAL biosynthesis.

pksT-2 generated another subclade with very strong bootstrap values (99%; Fig. 4) close to the fungal reducing PKS clade IV. These homologous clones also contain the same domain organization as KS-AT-DH-ER-KR-ACP in the type I PKS genes. Phylogenetic analysis using the amino acid sequences of the KS domain revealed that *pksT-2* is most closely related to the putative PKS from *T. vires* (86% sequence identity; accession number EHK18438.1) and *G. moniliformis* (33% sequence identity; accession number AAR92218.1). The KS domain analysis showed that *pksT-2* may be involved in fumonisin production based on an analysis of the NaPDoS database. Reducing PKS subclade IV, and subclades I and II may or may not have a conserved methyltransferase domain. The only characterized PKS in this subclade was *G. moniliformis* FUM1, which contains the KS-AT-DH-(C-MT)-ER-KR-ACP domains and forms the linear PK precursor of the toxin fumonisin.³⁰ The FUM1 expression levels was highly correlated with fumonisins based on real-time RT-PCR, which suggests that real-time RT-PCR is suitable for studying the influence of abiotic and biotic factors on the expression of these genes.^{31,32} Cox et al.³³ found that the C-MeT domain transfers a methyl group after the first and second rounds of iteration, but it is inactive in the final round along with the ER domain. However, many of the predicted PKSs in the PKS clade producing reduced PKs have high divergence and presumably nonfunctional MT domains.²¹ *pksT-2* does not contain the C-MT domain compared with domains of *G. moniliformis* FUM1, which may synthesize a compound similar to the linear PK precursor of fumonisin.

The NCBI ENTREZ accession numbers of the 55 fungal PKS sequences and a FAS sequence from *G. gallus* are shown in abbreviations table.

Expression patterns of *pksT-1* and *pksT-2* genes

We studied the effect of *T. harzianum* 88 confrontation with different fungal pathogens (*S. sclerotiorum*, *R. solani* and *F. oxysporum*) in the mRNA levels of *pksT-1* and *pksT-2* to elucidate the *pksT* genes expression. In the present study, fungal pathogens induction of two genes was noticeably high in *T. harzianum* 88 compared with the untreated controls.

pksT-1 expression was highly upregulated by *S. sclerotiorum*, increasing 1.88-fold within 3 h and peaking at 4.74-fold within 6 h. The *pksT-1* expression was decreased at 12, 24 and 36 h after induction. Significant changes in *pksT-1* mRNA levels were observed when *T. harzianum* 88 was challenged with *S. sclerotiorum* ($p \leq 0.01$). *R. solani* challenge induced the highest *pksT-1* mRNA levels at 1.22-fold within 3 h. However, the *pksT-1* mRNA levels decrease after 6, 12, 24 and 36 h, and the lowest level was observed at 12 h. These significant changes in *pksT-1* mRNA levels were also observed when *T. harzianum* 88 was challenged with *R. solani* ($p \leq 0.01$). *pksT-1* was also upregulated 1.07-fold by the *F. oxysporum* challenge compared with the untreated control at 3 h, but the increase was not statistically significant ($p > 0.05$). The increases in *pksT-1* expression at 6 h and at 12 h were significant, reaching its peak at 3.42-fold after 24 h, and significantly decreasing after 36 h ($p \leq 0.05$; Fig. 5A).

The *S. sclerotiorum*-induced *pksT-2* expression increased to almost 0.8-fold compared with the untreated samples at 3 h. The *pksT-2* expression decreased after 6 h, but increase from 12 h to 36 h ($p < 0.05$; Fig. 5B). We also observed the highest increase in *pksT-2* expression (1.33-fold) at 6 h after *R. solani* challenge ($p < 0.05$; Fig. 5B). Similarly, *F. oxysporum* increased *pksT-2* expression by ~0.93-fold compared with the untreated samples ($p < 0.05$ at 3, 6, 12, 24 and 36 h; Fig. 5B). The RT-qPCR analysis showed that the fungal pathogens induce *pksT-2* gene expression. In summary, fungal pathogens induce the transcription of *pksT* genes in *T. harzianum* 88.

These results were similar to that of numerous polyketide synthases, which are upregulated in creeping bentgrass infected with *Sclerotinia homoeocarpa*.³⁴ By contrast, the PcPKS2 transcript levels in the leaves are highly upregulated by pathogens.³⁵ 6msas activates disease resistance pathways by enhancing the accumulation of PR proteins and resistance to tobacco mosaic virus.³⁶ PKS/non-ribosomal peptide synthetase (NRPS) hybrid enzyme is also involved in *Trichoderma*-plant interactions that induce defence responses.³⁷ In addition, *T. harzianum* is a mycoparasitic filamentous fungus that produces several antifungal compounds when challenged with fungal pathogens to contribute to fungistasis. These antifungal compounds may participate in the biocontrol mechanism of *Trichoderma*.

In addition, PKS expression in fungi has not been studied in relation to pathogenesis and *Trichoderma*. The results indicate that with at least one of the three fungal pathogens causes the differential regulation of the two PKS genes. However, these genes generally display different expression patterns when *Trichoderma* encounters different fungal pathogens, which suggests that *T. harzianum* generates specific response patterns to different challenges.

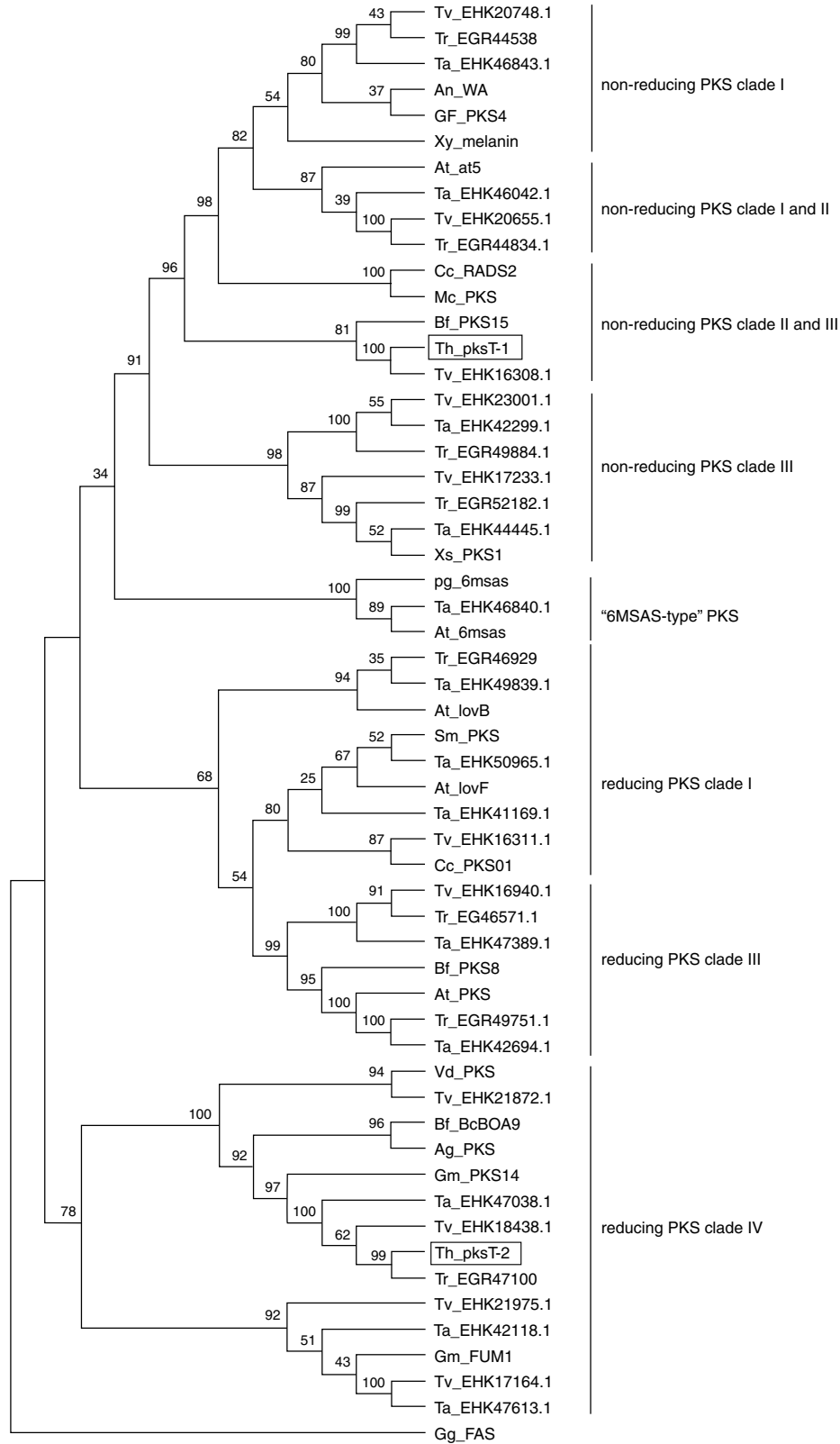


Fig. 4 – Relationship of *T. harzianum* 88 PKSs to fungal type I iterative PKSs. The tree was constructed with type I iterative PKS protein sequences. β -Ketoacyl synthase of *G. gallus* FAS was used as the out-group. A multiple sequence alignment was performed using the CLUSTALW (1.83) program, and the tree was generated with the MEGA (4.0) program. The indicated scale represents 0.1 amino acid substitution persite. PKSs of *T. harzianum* 88 are indicated in bold and framed with rectangles. Abbreviations, genus and species names and the NCBI ENTREZ accession numbers of the 55 fungal PKS sequences and the FAS sequence from *G. gallus* are given in abbreviation table.

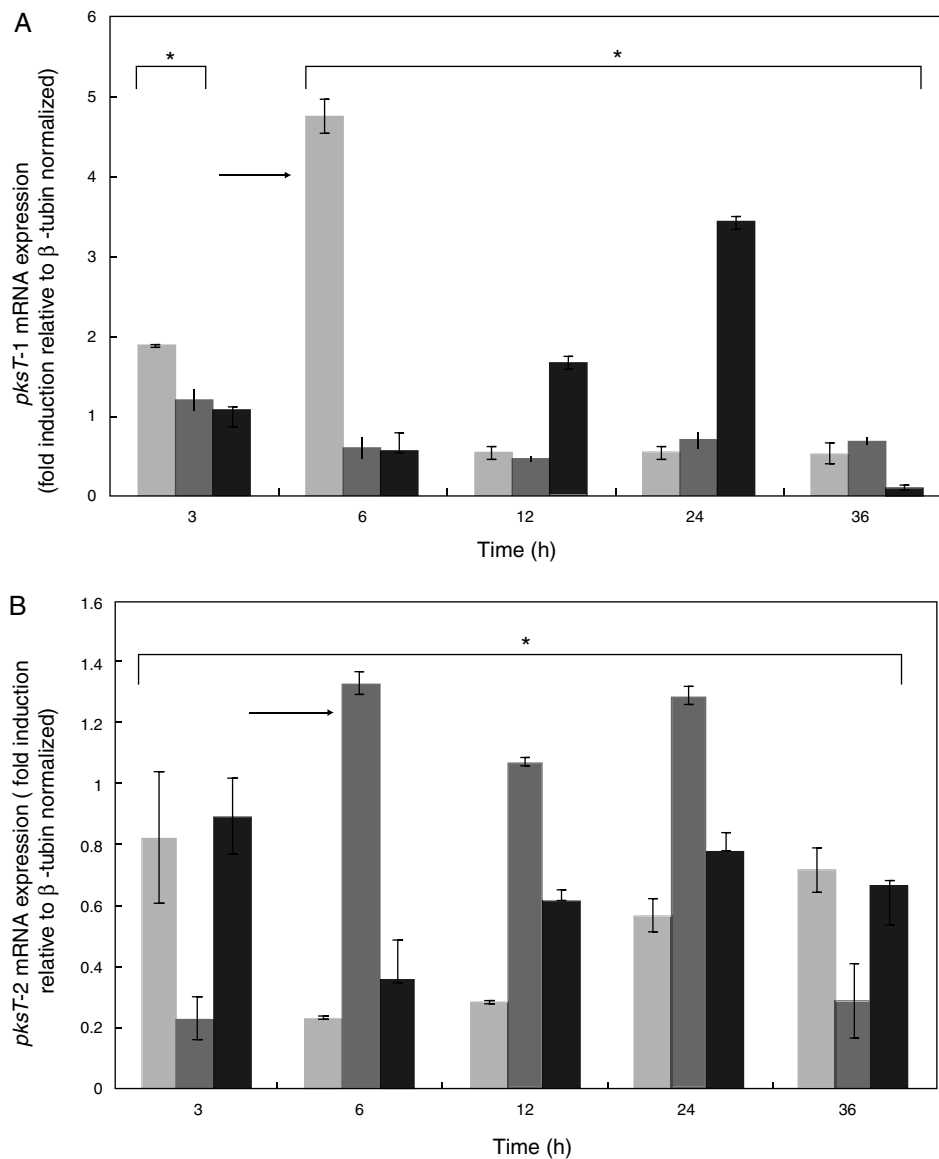


Fig. 5 – Time course expression analyses of PKS genes responding to confrontation with *R. solani*, *S. sclerotiorum* or *F. oxysporum*. X-axis: time points of confrontation with phytopathogens; Y-axis: mRNA expression (fold induction relative to β -tubulin normalized). The fold change in PKS gene expression was calculated using the formula $2^{-\Delta\Delta CT}$. White bars: expression responding to *S. sclerotiorum*; horizontal bars: expression responding to *R. solani*; Black bars: expression responding to *F. oxysporum*. *Significant difference at 0.05 level ($p < 0.05$) by comparing *T. harzianum* 88 which was confrontation with three fungal plant pathogens and non- confrontation with three fungal plant pathogens. Arrows indicate the highest expression of PKS genes responding to different phytopathogens.

Construction of the $\Delta pksT-2$ disruptant strain

The effect of the hygromycin B dose on the regeneration frequency of conidia was determined before transformation. Hygromycin B at 100 $\mu\text{g}/\text{mL}$ completely inhibited the regeneration of untransformed protoplasts. Therefore, growth at this concentration was used as the selection criterion for hygromycin B-tolerant transformants (Fig. 6).

We constructed a $\Delta pksT-2$ disruptant strain to examine the function of *pksT-2* in *T. harzianum*. *A. tumefaciens*-mediated

transformation obtained six candidate colonies. Subsequently, these colonies were screened via colony PCR using the primers $\Delta pksT-2$ check R and $\Delta pksT-2$ check F (Online Resource 1). We further confirmed the $\Delta pksT-2$ disruptant strain through Southern blot analysis. These analyses revealed the expected hybridization signal at 7.8 kb and at 6.5 kb in the digested genomic DNA isolated from the wild-type *T. harzianum* 88 and the $\Delta pksT-2$ candidate transformant with *Bgl*II (Fig. 6). These results indicate successful gene replacement at the resident $\Delta pksT-2$ locus.

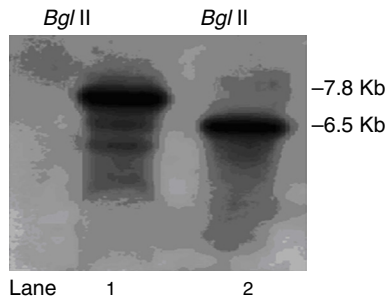


Fig. 6 – Southern blot analysis of genomic DNA from *pksT-2* disruptant and *T. harzianum* 88 digested with *Bgl* II as indicated. Bands were detected with $\Delta pksT-2-S$ (Lane 1, 2) digoxigenin-labelled probes.

Characterization of the *pksT-2* disruptant strain

We examined the *pksT-2* disruptant strain to determine its growth characteristics. Cell dry weight of wild-type and *pksT-2* disruptant strains increased with incubation time, and which of wild type *T. harzianum* 88 reached the highest weight at 84 h. However, based on the data obtained from the cell growth curves of *T. harzianum* 88 strain in our lab (data not shown), its cell has entered a decline phase at 108 h, At this point the cell dry weight is slightly lower at 108 h than at 84 h. Furthermore, cell dry weight of *pksT-2* disruptant strain growth slower than wild type *T. harzianum* 88, and which reached the highest weight at 108 h, but only 33% of the dry weight of the wild-type strain cell. The result showed that the growth rate of the strain harbouring the *pksT-2* disruptant on solid and liquid media was significantly lower than that of the wild-type strain (Fig. 7).

Phenotype of the *pksT-2* disruptant strain

We observed the phenotype of the *pksT-2* disruptant strain to confirm the function of *pksT-2* and to evaluate the gene targeting efficiency. *T. harzianum* 88 produced green conidia (Fig. 8A).

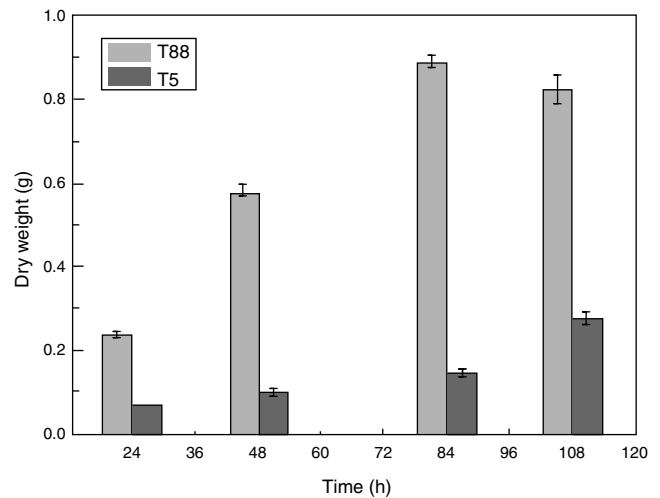


Figure 7 – Growth rates of the wild-type strain and *pksT-2* disruptant. The wild-type strain and *pksT-2* disruptant were inoculated in liquid MM medium (1×10^6 conidia/mL) and grown at 28 °C for 24, 48 h and 72 h, 150 rpm/min respectively. The data represent the mean \pm S.D ($n = 3$). Black bar: wild-type; white bar: *pksT-2* disruptant.

Under the same growth conditions *T. harzianum* 88 harbouring the *pksT-2* disruptant strain displayed a pink conidial phenotype (Fig. 8 B), and the yellow conidiation spread into solid medium. This result indicates that inactivation of the *pksT-2* gene influences the conidial pigmentation of *T. harzianum* 88. Polyketides are involved in the biosynthesis of important natural products, such as fungal pigments,³⁸ antibiotics, and a variety of therapeutic compounds.³⁹ The function of a number of genes in *T. harzianum* 88 genomic DNA that are involved in secondary metabolic pathways, such as PKS and NRPS are unknown. Thus, *T. harzianum* 88 with the *pksT-2* disruptant will be useful for gene disruption experiments to analyse gene function.

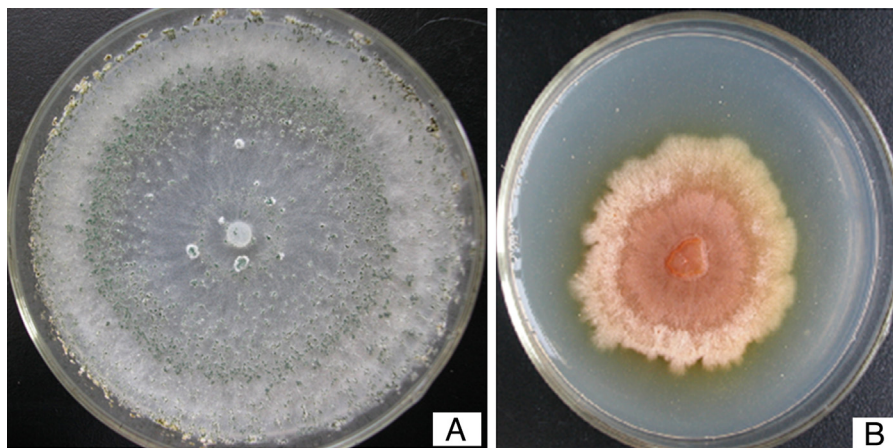


Fig. 8 – Generation of a *pksT-2* disruptant. Phenotype of the *pksT-2* disruptant grown on MM agar at 28 °C for 3 days. The wild strain displayed the typical green conidia (A) and the *pksT-2* disruptant displayed pink conidia (B).

Conclusions

In conclusion, *pksT-1* and *pksT-2* were isolated from *T. harzianum* 88. Although secondary metabolites are unrelated to *pksT-1* and *pksT-2*, analysis of their domain organization implied that *pksT-1* provides a side chain in RAL biosynthesis and *pksT-2* is involved in compound biosynthesis similar to fumonisin biosynthesis. The expression levels of the *pksT-1* and *pksT-2* genes were evaluated via real-time RT-PCR during challenge with different fungal pathogens (*S. sclerotiorum*, *R. solani* and *F. oxysporum*). The results indicated that *pksT-1* and *pksT-2* are differentially regulated when *T. harzianum* 88 is challenged with at least one of three fungal pathogens. A *pksT-2* disruptant strain was obtained through gene functional inactivation, and its growth rate was slower than that of the wild type. The *pksT-2* disruptant strain showed that the *pksT-2* gene encodes a key enzyme which may be involved with pigmentation.

Future studies will focus on the heterologous expression of *pksT-1* and *pksT-2* to confirm their functions. These studies will provide a basis for the sustainable application of *T. harzianum* 88 secondary metabolites in pharmaceutical treatment and biocontrol of plant pathogens.

Conflicts of interest

The authors declare no conflicts of interest.

Acknowledgment

Project supported by the National Science Foundation for Distinguished Young Scholars of China (Grant No. 31501839).

Appendix A. Supplementary data

Supplementary data associated with this article can be found, in the online version, at [doi:10.1016/j.bjm.2016.01.004](https://doi.org/10.1016/j.bjm.2016.01.004).

REFERENCES

- Gilardi G, Baudino M, Gullino ML, Garibaldi A. Attempts to control *Fusarium* root rot of bean by seed dressing. *Commun Agric Appl Biol Sci*. 2008;73:75–80.
- Martínez-Medina A, Pascual JA, Pérez-Alfocea F, Albacete A, Roldán A. *Trichoderma harzianum* and *Glomus intraradices* modify the hormone disruption induced by *Fusarium oxysporum* infection in melon plants. *Phytopathology*. 2010;100:682–688.
- Cheng CH, Yang CA, Peng KC. Antagonism of *Trichoderma harzianum* ETS 323 on *Botrytis cinerea* mycelium in culture conditions. *Phytopathology*. 2012;102:1054–1063.
- Huang X, Chen L, Ran W, Shen Q, Yang X. *Trichoderma harzianum* strain SQR-T37 and its bio-organic fertilizer could control *Rhizoctonia solani* damping-off disease in cucumber seedlings mainly by the mycoparasitism. *Appl Microbiol Biotechnol*. 2011;91:741–755.
- Naeimi S, Kocsubé S, Antal Z, et al. Strain-specific SCAR markers for the detection of *Trichoderma harzianum* AS12-2, a biological control agent against *Rhizoctonia solani*, the causal agent of rice sheath blight. *Acta Biol Hung*. 2011;62:73–84.
- Lo CT, Nelson EB, Hayes CK, Harman GE. Ecological studies of transformed *Trichoderma harzianum* strain 1295-22 in the rhizosphere and on the phylloplane of creeping bentgrass. *Phytopathology*. 1998;88:129–136.
- Amer MA, Abou-El-Seoud II. Mycorrhizal fungi and *Trichoderma harzianum* as biocontrol agents for suppression of *Rhizoctonia solani* damping-off disease of tomato. *Commun Agric Appl Biol Sci*. 2008;73:217–232.
- Kim TG, Knudsen GR. Comparison of real-time PCR and microscopy to evaluate sclerotial colonisation by a biocontrol fungus. *Fungal Biol*. 2011;115:317–325.
- Kroken S, Glass NL, Taylor JW, Yoder OC, Turgeon BG. Phylogenomic analysis of type I polyketide synthase genes in pathogenic and saprobic ascomycetes. *Proc Natl Acad Sci U S A*. 2003;100:15670–15675.
- Schuster A, Schmoll M. Biology and biotechnology of *Trichoderma*. *Appl Microbiol Biotechnol*. 2010;87:787–799.
- Harman GE, Petzoldt R, Comis A, Chen J. Interactions between *Trichoderma harzianum* strain T22 and maize inbred line Mo17 and effects of these interactions on diseases caused by *Pythium ultimum* and *Colletotrichum graminicola*. *Phytopathology*. 2004;94:147–153.
- Shoresh M, Harman GE. The relationship between increased growth and resistance induced in plants by root colonizing microbes. *Plant Signal Behav*. 2008;3:737–739.
- Tucci M, Ruocco M, De Masi L, De Palma M, Lorito M. The beneficial effect of *Trichoderma* spp. on tomato is modulated by the plant genotype. *Mol Plant Pathol*. 2011;12:341–354.
- Zeilinger S, Omann M. *Trichoderma* biocontrol: signal transduction pathways involved in host sensing and mycoparasitism. *Gene Regul Syst Biol*. 2007;1:227–234.
- Moreno-Mateos MA, Delgado-Jarana J, Codón AC, Benítez T. pH and Pac1 control development and antifungal activity in *Trichoderma harzianum*. *Fungal Genet Biol*. 2007;44:1355–1367.
- Sempere F, Santamarina MP. In vitro biocontrol analysis of *Alternaria alternata* (Fr.) Keissler under different environmental conditions. *Mycopathologia*. 2007;163:183–190.
- Vinale F, Ghisalberti EL, Sivasithamparan K, et al. Factors affecting the production of *Trichoderma harzianum* secondary metabolites during the interaction with different plant pathogens. *Lett Appl Microbiol*. 2009;48:705–711.
- Hannan MA, Hasan MM, Hossain I, Rahman SM, Ismail AM, Oh DH. Integrated management of foot rot of lentil using biocontrol agents under field condition. *Microbiol Biotechnol*. 2012;22:883–888.
- Hertweck C. The biosynthetic logic of polyketide diversity. *Angew Chem Int Ed Engl*. 2009;48:4688–4716.
- Cox RJ. Polyketides, proteins and genes in fungi: programmed nano-machines begin to reveal their secrets. *Org Biomol Chem*. 2007;5:2010–2026.
- Chiang YM, Oakley BR, Keller NP, Wang GC. Unraveling polyketide synthesis in members of the genus *Aspergillus*. *Appl Microbiol Biotechnol*. 2010;86:1719–1786.
- Amnuaykanjanasin A, Punya J, Paungmoung P, et al. Diversity of type I polyketide synthase genes in the wood-decay fungus *Xylaria* sp. BCC 1067. *FEMS Microbiol Lett*. 2005;251:125–136.
- Wei Q, ed. *The guide of molecular biology experiment*. Harbin: Higher Education Publishing; 2007.
- Carsolio C, Gutiérrez A, Jiménez B, Van Montagu M, Herrera-Estrella A. Characterization of ech-42, a *Trichoderma harzianum* endochitinase gene expressed during mycoparasitism. *Proc Natl Acad Sci U S A*. 1994;91:10903–10907.
- Liu Z, Yang X, Sun D, et al. Expressed sequence tags-based identification of genes in a biocontrol strain *Trichoderma asperillum*. *Mol Biol Rep*. 2010;37:3673–3681.

26. Livak KJ, Schmittgen TD. Analysis of relative gene expression data using real-time quantitative PCR and the 2-delta delta CT method. *Methods*. 2001;25:405–408.
27. Gardiner DM, Howlett BJ. Negative selection using thymidine kinase increases the efficiency of recovery of transformants with targeted genes in the filamentous fungus *Leptosphaeria maculans*. *Curr Genet*. 2004;45:249–255.
28. Baker SE, Perrone G, Richardson NM, Gallo A, Kubicek CP. Phylogenomic analysis of polyketide synthase-encoding genes in *Trichoderma*. *Microbiology*. 2012;158(pt 1):147–154.
29. Wang S, Xu Y, Maine EA, et al. Functional characterization of the biosynthesis of radicicol, an Hsp90 inhibitor resorcylic acid lactone from *Chaetomium chiversii*. *Chem Biol*. 2008;15:1328–1338.
30. Sagaram US, Shim WB. *Fusarium verticillioides* GBB1, a gene encoding heterotrimeric G protein beta subunit, is associated with fumonisin B biosynthesis and hyphal development but not with fungal virulence. *Mol Plant Pathol*. 2007;8:375–384.
31. De Oliveira Rocha L, Reis GM, da Silva VN, Braghini R, Teixeira MM, Corrêa B. Molecular characterization and fumonisin production by *Fusarium verticillioides* isolated from corn grains of different geographic origins in Brazil. *Int J Food Microbiol*. 2011;145:9–21.
32. Menendez AB, Godeas A. Biological control of *Sclerotinia sclerotiorum* attacking soybean plants. Degradation of the cell walls of this pathogen by *Trichoderma harzianum* (BAFC 742). Biological control of *Sclerotinia sclerotiorum* by *Trichoderma harzianum*. *Mycopathologia*. 1998;142:153–160.
33. Cox RJ, Glod F, Hurley D, et al. Rapid cloning and expression of a fungal polyketide synthase gene involved in squalenol biosynthesis. *Chem Commun (Camb)*. 2004:2260–2261.
34. Mitchell T, Boehm M, Hu JN, Venu RC. Identification of potential pathogenicity factors and host defense genes in the *Sclerotinia homoeocarpa*–turfgrass pathosystem using transcriptome analysis. In: *Proc. ASA, CSSA and SSSA Annual Meetings*. 2011.
35. Ma LQ, Pang XB, Shen HY, et al. A novel type III polyketide synthase encoded by a three-intron gene from *Polygonum cuspidatum*. *Planta*. 2009;229:457–469.
36. Yalpani N, Altier DJ, Barbour E, Cigan AL, Scelonge CJ. Production of 6-methylsalicylic acid by expression of a fungal polyketide synthase activates disease resistance in tobacco. *Plant Cell*. 2001;13:1401–1409.
37. Mukherjee PK, Buensanteai N, Moran-Diez ME, Druzhinina IS, Kenerley CM. Functional analysis of non-ribosomal peptide synthetases (NRPSs) in *Trichoderma virens* reveals a polyketide synthase (PKS)/NRPS hybrid enzyme involved in the induced systemic resistance response in maize. *Microbiology*. 2012;158(pt 1):155–165.
38. Rugbjerg P, Naesby M, Mortensen UH, Frandsen RJ. Reconstruction of the biosynthetic pathway for the core fungal polyketide scaffold rubrofusarin in *Saccharomyces cerevisiae*. *Microb Cell Fact*. 2013;12:31.
39. Dasgupta A. Advances in antibiotic measurement. *Adv Clin Chem*. 2012;56:75–104.